Ecological Informatics 31 (2016) 100–111

Contents lists available at ScienceDirect

Ecological Informatics

journal homepage: www.elsevier.com/locate/ecolinf

Challenges and opportunities in synthesizing historical geospatial data using statistical models

M.V. Eitzel [a,*], Maggi Kelly [a], Iryna Dronova [b], Yana Valachovic [c], Lenya Quinn-Davidson [c], Jon Solera [d], Perry de Valpine [a]

[a] Department of Environmental Science, Policy, and Management, University of California, Berkeley, 130 Mulford Hall #3114, Berkeley, CA 94720-3114, USA
[b] Department of Landscape Architecture and Environmental Planning, University of California, Berkeley, 230 Wurster Hall #1820, Berkeley, CA 94720-1820, USA
[c] University of California Cooperative Extension, 5630 South Broadway, Eureka, CA 95503, USA
[d] Seven Points Consulting, 900 San Bruno Ave, Brisbane, CA 94005, USA

ARTICLE INFO

Article history:
Received 4 October 2015
Received in revised form 17 November 2015
Accepted 23 November 2015
Available online 2 December 2015

Keywords:
Spatial autocorrelation
Object-Based Image Analysis
Definiens
Black and white images
Scaling
Generalized Additive Models

ABSTRACT

We classified land cover types from 1940s historical aerial imagery using Object Based Image Analysis (OBIA) and compared these maps with data on recent cover. Few studies have used these kinds of maps to model drivers of cover change, partly due to two statistical challenges: 1) appropriately accounting for spatial autocorrelation and 2) appropriately modeling percent cover which is bounded between 0 and 100 and not normally distributed. We studied the change in woody cover at four sites in California's North Coast using historical (1948) and recent (2009) high spatial resolution imagery. We classified the imagery using eCognition Developer and aggregated the resulting maps to the scale of a Digital Elevation Model (DEM) in order to understand topographic drivers of woody cover change. We used Generalized Additive Models (GAMs) with a quasi-binomial probability distribution to account for spatial autocorrelation and the boundedness of the percent woody cover variable. We explored the relative influences on current percent woody cover of topographic variables (grouped using principal component analysis) reflecting water retention capacity, exposure, and within-site context, as well as historical percent woody cover and geographical coordinates. We estimated these models for pixel sizes of 20, 30, 40, 50, 60, 70, 80, 90, and 100 m, reflecting both tree neighborhood scales and stand scales. We found that historical woody cover had a consistent positive effect on current woody cover, and that the spatial autoregressive term in the model was significant even after controlling for historical cover. Specific topographic variables emerged as important for different sites at different scales, but no overall pattern emerged across sites or scales for any of the topographic variables we tested. This GAM framework for modeling historical data is flexible and could be used with more variables, more flexible relationships with predictor variables, and larger scales. Modeling drivers of woody cover change from historical ecology data sources can be a valuable way to plan restoration and enhance ecological insight into landscape change.

1. Introduction

Historical ecology is a flourishing interdisciplinary area of study concerned with the reconstruction of landscapes from decades to centuries ago, often for the purpose of setting restoration targets (Grossinger, 2012; Sanderson, 2009; Swetnam et al., 1999). Increasingly, the field is shifting from descriptions for restoration targets to include quantitative modeling of long term landscape change (Whipple et al., 2011). This development allows historical ecology to contribute to current understandings of the long term effects of global change. Our goal with this study was to explore the challenges and opportunities inherent in the quantitative modeling of historical ecological data using relatively easily available datasets, and to investigate ways to assess the validity of the resulting models in the absence of ground-truth information. We used these methods to investigate vegetation change (specifically, forest densification) in coastal Northern California.

We used quantitative modeling of woody cover change from historical imagery to ask and answer questions regarding the topographic determinants of forest densification. The process of densification has many undesirable consequences for forest ecosystem services, such as increased fuel continuity and subsequent fire hazard, decreased

Abbreviations: OBIA, Object-Based Image Analysis; DEM, Digital Elevation Model; GAM, Generalized Additive Model; NAIP, National Agricultural Imagery Program; NDVI, Normalized Difference Vegetation Index; GLCM, Gray-level Co-occurrence Matrix; MRF, Markovian Random Field; GIS, Geographic Information Systems; RMSE, Root Mean Squared Error.

* Corresponding author at: Science and Justice Research Center, University of California, Santa Cruz, 1156 High St., Santa Cruz, CA 95064, USA. Tel.: +1 831 459 3837; fax: +1 831 459 3518.
E-mail address: mveitzel@ucsc.edu (M.V. Eitzel).

http://dx.doi.org/10.1016/j.ecoinf.2015.11.011

heterogeneity and decreased resiliency, decreases in biodiversity due to decreased light availability on the forest floor, and compromised tree health due to more intense resource competition (Hanberry et al., 2014; Knapp et al., 2013). This process is widespread in California due to fire exclusion policies dating back more than 100 years (Laudenslayer and Darr, 1990). Topographic variables representing water retention capacity and exposure (including slope, aspect, elevation, curvature, solar radiation, and topographic wetness index) have long been used to predict vegetation characteristics (Deng et al., 2007; Franklin, 1995; Jenkins and Coops, 2011). Though they themselves are static, topographic variables can reflect underlying drivers such as solar exposure and moisture accumulation, which could modify the dynamic effects of climate change on cover. Many of these variables are easily calculated from a Digital Elevation Model (DEM) and are often used in GIS modeling studies. Our goal was to model the topographic determinants of current woody cover while using historical woody cover from aerial photographs to account for historical conditions, and to compare the importance of these factors in predicting current woody cover.

Historical aerial imagery, typically dating back to the 1930s and 1940s, is available throughout North America (Morgan and Gergel, 2013) and is often an important data source for historical ecology. Though the imagery can be difficult to find and often requires extensive pre-processing, classification of high spatial resolution black-and-white images has become more common with the commercial availability of Object Based Image Analysis (OBIA) software. OBIA allows analysts to use textural and contextual information in classifying single band images, and the use of OBIA with historical aerial photos has expanded in the last 10 years (Allard et al., 2012; Laliberte et al., 2004; Marignani et al., 2008; Martha et al., 2012; Pringle et al., 2009). Generally speaking, most of the OBIA change detection literature is focused on innovations in mapping techniques and their application to many different systems (Conchedda et al., 2008; de Chant and Kelly, 2009; Desclée et al., 2006; Dronova et al., 2011; Stow et al., 2008). The new goal, however, is not just to map the change but to understand the drivers of the mapped change, an interdisciplinary project involving both modeling and historical ecology (Gimmi and Bugmann, 2013). Among studies using OBIA to classify historical aerial imagery, only a few model the drivers of change (Cserhalmi et al., 2011; Garbarino et al., 2013; Levick and Rogers, 2011; Newman et al., 2014a,2014b; Platt and Schoennagel, 2009).

One issue that arises in combining historical aerial imagery with DEM-derived topographic variables is the problem of scale mismatch between ecological processes and data sources as well as between different data sources. Though geospatial data are becoming available on finer and finer spatial scales, the available data are often at an arbitrary resolution that is more constrained by data acquisition than the process of interest (Deng et al., 2007). Different ecological processes may act at different spatial scales (i.e., raster cell sizes) and different hierarchical organization levels (e.g., individual tree, neighborhood, stand, site, landscape). For instance, a tree may compete for light with other trees in its immediate neighborhood, but moisture accumulation may be a feature of the topography underlying an entire stand of trees. These hierarchical levels may not match spatial scales, and thresholds in the importance of different variables may appear where emergent properties arise (Bissonette, 1997). Ecologically, it would be ideal to explore the effects of densification at multiple levels of the hierarchy, from the tree neighborhood to the forest stand. Recent efforts to study changing forest responses at multiple spatial scales use simulation as a way to achieve this goal (Seidl et al., 2013). Empirical studies on scaling relationships for vegetation patterns so far have only correlated topographic variables with vegetation indices at a range of spatial scales rather than testing multiple variables at once while incorporating spatial autocorrelation (Deng et al., 2007). Methodologically, there is a need for data driven ecosystem modeling using appropriate statistical models and especially for scale sensitivity analysis of these models. Parameters for variables that are clearly important will theoretically be consistent in magnitude, direction, and significance for a range of cell sizes within an ecological scale. Parameter instability over a small range of cell sizes may indicate sensitivity to the particulars of the dataset. We therefore conducted our analysis at a range of cell sizes in order to assess scale-sensitivity.

In this study, we used object based image analysis on high spatial resolution images to map 1948 (historical) and 2009 (recent) woody cover at four sites in northern California, USA. We modeled recent cover as a function of topographic variables and historical cover using a quasi-binomial Generalized Additive Model (GAM) with a nonparametric smooth function of the spatial coordinates. We used these models at a range of raster cell sizes to answer the following questions:

1. Did woody cover increase more at wetter sites (those with higher annual rainfall)?
2. Did variables representing water retention capacity, exposure, and local context within the site demonstrate significant and ecologically reasonable relationships with recent woody cover, after controlling for historical woody cover?
3. Were these relationships stronger at the neighborhood scale or at the stand scale, and was a threshold effect apparent between the two scales (Fig. 1)?
4. Were these results stable over several cell sizes within an ecological scale?

2. Methods

2.1. Study areas

Four research sites were established in Northern California, primarily in Humboldt County. The sites have a Mediterranean climate, with cool, wet winters and hot, dry summers. Oak woodlands at our sites in Humboldt County are characterized by California black oak (*Quercus kelloggii*) and Oregon white oak (*Quercus garryana*) with an understory predominantly composed of grasses and forbs. Densification from woodland (defined as more than 30% cover with 150–300 trees/ha, Agee, 1993) to closed canopy forest (greater than 300 trees/ha, Agee, 1993) can occur when mature oak canopies expand through annual growth, but it more commonly occurs when evergreen species, typically Douglas-fir (*Pseudotsuga menziesii*), encroach into woodlands over time, forming a dense, shaded forest with little to no herbaceous understory. This represents an ecosystem type change with many consequences for biodiversity, forage production, and fire behavior (Engber et al., 2011; Livingston, 2014; Thysell and Carey, 2001). Our sites were chosen to represent several different latitudes and distances from the coast where densification was known to occur: Iaqua Buttes, Bald Hills, Willow Creek, and Blake Mountain (Fig. 2, Table 1). Analysis polygons within

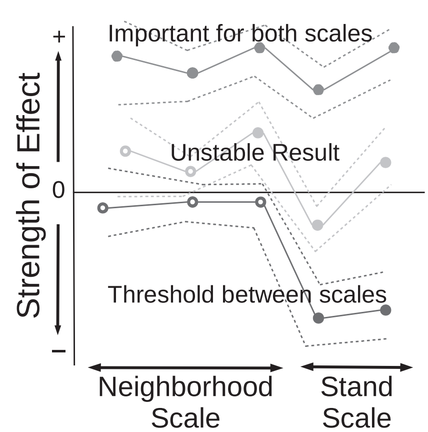

Fig. 1. Diagram of scaling effects. Dashed lines show confidence intervals, solid dots are significant, while hollow dots are not significant (confidence interval overlaps zero). Each dot is a raster cell size. Some parameters may be important for both scales, while others show instability from scale to scale; and still others might indicate a threshold of importance between the two scales indicating the potential for an emergent property.

sites were designed to capture a gradient of primarily Douglas-fir-caused densification and to avoid areas with active management by harvest or fire. We further adjusted the study boundary polygons to remove artifacts such as marks on the historical images.

2.2. Imagery and data sources

Historical images were flown for the USDA Forest Service in 1948. The black and white (panchromatic) image frames were later scanned by the California Department of Forestry and Fire Protection Humboldt-Del Norte Unit at 800 dots per inch, which after orthorectification resulted in one meter by one meter square pixels. For the analysis, we used frames CDF2-17-007 (Iaqua Buttes), CDF2-15-093 (Blake Mountain), CDF2-15-153 (Willow Creek), and CDF2-19-196 (Bald Hills). For image pre-processing, we also used neighboring frames in each flightline, though these additional images were not included in this analysis. Metadata was available for these flights at the UC Santa Barbara Map Library.[1]

Our recent images were from the 2009 survey of the US Department of Agriculture's National Agricultural Imagery Program (NAIP), as downloaded and tiled by Cal-Atlas.[2] NAIP is high spatial resolution (1-m × 1-m pixels) and has four bands: red (~635 nm), green (~560 nm), blue (~460 nm), and near infra-red (~860 nm). NAIP imagery is already orthorectified and projected to Universal Transverse Mercator (UTM) Zone 10 N.

The digital elevation model (DEM) was obtained from USGS' National Elevation Dataset, as downloaded and tiled by Cal-Atlas.[3].We projected the DEM to UTM zone 10 N coordinates, and used it both for orthorectification and for calculating topographic predictor variables. The topographic variables we included in our models were the following:

1. Elevation from the DEM in meters
2. Topographic slope in degrees (maximum change in elevation between a cell and any of its neighboring cells)
3. Curvature (second derivative of elevation, maximum change in any direction)
4. Plan curvature (in the direction of no change in elevation)
5. Profile curvature (in the direction of steepest descent/ascent)
6. 'Northness,' the cosine of aspect (measured from north, with '1' indicating north and '−1' indicating south) and
7. 'Eastness,' the sine of aspect ('1' indicating east and '−1' indicating west) as used in (Levick and Rogers, 2011)
8. 'Heat load index,' calculated as $1 - cos(\theta - 45) / 2$ where θ is the aspect in degrees (Stoddard and Hayes, 2005)
9. Solar radiation (insolation) as calculated in ArcGIS's solar radiation calculator (ESRI, 2013)
10. Distance to the nearest ridge (using the 'flowdir' tool in ArcGIS)
11. Distance to the 'prairie' class (reflecting the distance to the forest edge; using the 'Near' tool in ArcGIS)
12. Topographic wetness index (sometimes referred to as topographic moisture index or compound topographic index). Topographic wetness index was defined as $ln(\alpha/tan(\beta))$. In this equation, α was the catchment area collecting to that pixel (offset by one in order to avoid taking the log of zero), calculated from a watershed delineation tool and divided by the cell width; and β was the slope in degrees (see Supplementary data for ArcGIS calculation of topographic wetness index in Python script). Topographic wetness index has been shown to explain variation in vegetation metrics (Jenkins and Coops, 2011; Wang et al., 2013).

[1] http://mil.library.ucsb.edu/apcatalog/report/report.php?filed_by=CDF2.
[2] http://www.atlas.ca.gov/download.html#/casil/imageryBaseMapsLandCover/imagery/naip.
[3] http://www.atlas.ca.gov/download.html#/casil/elevation.

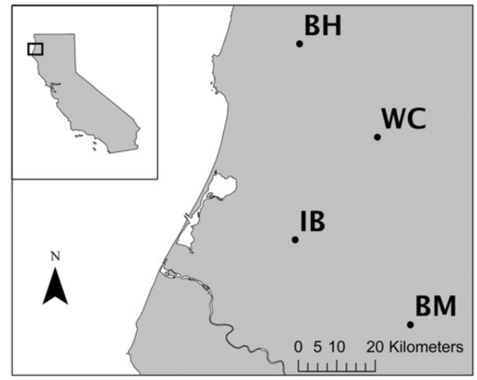

Fig. 2. Geographical context. The four sites (Iaqua Buttes — IB; Bald Hills — BH; Blake Mountain — BM; Willow Creek — WC) are located primarily in upper Humboldt County in California, USA.

Many of our topographic variables were collinear, in some cases due to a direct mathematical relationship (e.g., northness and heat load index). Many strategies have been proposed for ways to make principled choices of collinear variables or ways to combine them (Dormann et al., 2013). We addressed this issue using a principal component analysis to create combinations of variables: water retention capacity-related variables (curvature, plan curvature, profile curvature, topographic wetness index, and topographic slope), exposure-related variables (northness, eastness, heat index, and solar radiation), and 'local context' variables that reflected the position of the cell relative to other parts of the site (distance to the nearest ridge, distance to the 'prairie' class, and elevation). We flipped the sign of some of these variables to create combinations that reflected a hypothesized increase in moisture (and therefore cover); this results in hypothesized positive parameter estimates for slopes for these grouped variables. We did this grouping independently at each scale and for each site. We used the first component of each of the three groups. This procedure resulted in three predictor variables, which typically accounted for at least 50% of the variation in their respective groups (Appendix A). We also included historical woody cover as a separate fourth predictor variable. Note that for Willow Creek, there was no prairie near the analysis polygon so that variable is not included in the 'local context' group for that site.

Raster operations and calculations were conducted in ArcGIS 10.2 (ESRI, 2013); see Supplementary data for Python scripts. Topographic predictor variables were standardized (centered and scaled by their respective standard deviations) within each site/cell size combination in order to compare their relative impact on woody cover percentage. Based on the hypothesis that greater moisture enables greater growth for woody species, we predicted that northness would have a positive effect on woody cover, eastness would have a small but positive effect (as afternoon sun on west facing slopes is more drying than morning sun on eastern slopes, Deng et al., 2009), topographic moisture index

Table 1
Site characteristics.

	Bald Hills	Blake Mountain	Iaqua Buttes	Willow Creek
Distance from coast (km)	18.8	62.7	26.5	39.4
Average elevation (m)	585	1180	775	375
Latitude (°N)	41.17	40.51	40.71	40.95
Longitude (°W)	123.89	123.53	123.90	123.66
Total annual rainfall (mm)	2782	1588	1837	1458
July–August mean temperature (°C)	19.3	20.9	18.6	23.9

would have a positive effect, steeper slopes would have a negative effect, and positive curvature (defined in ArcGIS as convex upward) would have a negative effect on current cover. We hypothesized that historical cover would have a positive effect on current cover in all cases. We also hypothesized that distance from prairie would have a negative effect on cover, distance to ridge would have a positive effect, and elevation would have a positive effect. These three variables represent the distance to the forest edge ('prairie' class) or to the particular location of Douglas-fir at a given site. Because mature Douglas-fir trees are sources of a large volume of seed contributing strongly to densification processes at these sites, we expect variables which represent greater distances to those seed sources to predict less densification. Based on the location of the nearest mature Douglas-fir stands for each site (unpublished data), we would expect elevation to have a positive effect for Iaqua Buttes, Blake Mountain, and Bald Hills, and a negative effect for Willow Creek.

2.3. Pre-processing of imagery

We used Leica Photogrammetry Suite (Intergraph, 2012) to orthorectify and georegister the imagery using the 2009 NAIP imagery as a horizontal reference and the 10-m DEM as a vertical reference. We collected 50–150 ground control points for each site and used cubic convolution resampling for the orthorectification (see Supplementary data for instructions on orthorectification in LPS). We used ArcGIS (ESRI, 2013) to mask and mosaic the historical images to each site's polygon. We used package "glcm" (Zvoleff, 2014) in R (R Development Core Team, 2009) to calculate six different per-pixel gray-level co-occurrence matrix (GLCM) textures with a 7×7 moving window (Haralick et al., 1973). We calculated mean, variance, contrast, dissimilarity, entropy, and second moment. We chose a 7×7 window because it produced a visually smoother result, which was better for later segmentation and classification (see Supplementary data for R code to calculate texture layers). For the 2009 NAIP imagery, we calculated a per-pixel Normalized Difference Vegetation Index (NDVI) layer using ArcGIS's Raster Calculator to use in segmentation.

2.4. Segmentation and classification

We used eCognition Developer 8 (Trimble, 2013) to segment and classify each image for each site and year (total of eight images). Consistently automatically identifying species from historical imagery proved to be prohibitive (Eitzel et al., 2015), so our study was restricted to a more general assessment of densification measured through changes in woody versus herbaceous cover. This classification conflated densification due to expansion of oak canopies and densification due to encroachment of Douglas-fir. We used a simple classification scheme at two scales. Because we were interested in forest densification, we first classified land cover as 'forest' (characterized by dominance of woody species) or 'prairie' (characterized by open grassland area with very little tree canopy cover), and masked out 'prairie' according to the 2009 forest/prairie edge. There was little recruitment of woody species in the middle of the prairie, and any advancement of woody cover into the prairie at the forest edge between 1948 and 2009 was captured by using the 2009 image as the mask. Following this classification, within the 'forest' type, we classifed areas as 'woody' (oak, Douglas-fir, shrubs, or other trees) and 'herbaceous' (open clearings). We proceeded with analysis of 'woody' versus 'herbaceous' only within the 2009 'forest' area.

For the 2009 NAIP imagery, we used all four bands (R, G, B and IR) and per-pixel NDVI, and for historical imagery we used the image brightness and the six GLCM texture measures. We first used multiresolution segmentation with a large scale parameter to mask forest and prairie from each other, and then multi-threshold segmentation on various bands to classify within those areas (Gärtner et al., 2014). Using ArcGIS's 'classify' tool for raster symbology, we examined the histogram of values for the band in question for breakpoints in order to choose thresholds. Different bands were helpful for segmenting and classifying different images. For 2009 NAIP images, NDVI as well as mean values of different bands (e.g., green, infra-red), or overall image brightness were often helpful (and for one site, Bald Hills, per-pixel texture variables calculated for the red band in addition to the image bands and NDVI were needed in order to discriminate between classes); for historical imagery the image brightness value worked well, in addition to contrast, homogeneity, dissimilarity and second moment (see Supplementary data for example eCognition rule sets).

Ultimately we conducted further analysis of woody cover change on only the forest region. We also restricted the analysis to areas with no more than 5 m of offset in registration between the recent and historical images (estimated using the 'measurement' tool ArcGIS). This resulted in areas of 52 ha (Iaqua Buttes), 63 ha (Willow Creek), 71 ha (Bald Hills), and 77 ha (Blake Mountain).

2.5. Accuracy assessment

We assessed classification accuracy within the analysis regions for each image by selecting 100 random points using ArcGIS's random point generating utility and visually assessing the class at that point (see Supplementary data for Python code). Because herbaceous cover was much less common in the forested area, we used a proportionally stratified sampling strategy and ensured that at least 10 points of classified herbaceous cover were assessed for accuracy at each site. Preliminary accuracies were determined to be similar for individual sites, so we pooled the accuracy assessment across sites. We then generated an additional 15 random points within herbaceous cover for the 2009 images so the total across sites was more than 50.

Like most historical image classification studies, we lacked alternative imagery to validate the historical imagery, nor did we have alternative imagery to validate the recent high resolution imagery, and thus we verified the class by eye (looking at the neighborhood around the point and using additional cues such as ecological context to judge the actual class) to compare with the assigned class (Cserhalmi et al., 2011; Levick and Rogers, 2011; Platt and Schoennagel, 2009). In a few cases random points fell into pixels that were obviously mixed between herbaceous and woody cover (7 cases out of 815 points); these were thrown out due to the impossibility of assigning a class to the point. We considered accuracy assessment based on objects, but because multi-threshold segmentation results in few very large objects (unlike multi-resolution segmentation which results in fairly similarly sized objects due to the constraint of the scale parameter), there were no appropriate objects to sample from and we determined that a point-based accuracy assessment was best (Müllerová et al., 2013). We report standard accuracies and kappa values to enable comparison with other studies (Jensen, 2005; Müllerová et al., 2013).

2.6. Statistical models and scaling

The relative advantages and disadvantages inherent in different methods of accounting for spatial autocorrelation in statistical models have been much debated recently (Beale et al., 2010; Betts et al., 2009; Dormann, 2009; Dormann et al., 2007; Hawkins, 2012; Kuhn and Dormann, 2012; Miller et al., 2007). In addition, the issue of transforming or otherwise appropriately working with proportion data has been highlighted for a long time, with recent developments favoring binomial or beta distributions with logit link functions (Herpigny and Gosselin, 2015; Schmid et al., 2013; Warton and Hui, 2011).

We incorporated spatial autocorrelation in our models using a smooth function of geographical coordinates (UTM Northing and Easting) in a Generalized Additive Model (GAM) in the R package "mgcv"

(Mixed GAM Computation Vehicle; Wood, 2006). The GAM was ideal for these data for two reasons: 1) a Markovian random field (MRF) basis was available for the smoothing function, which is designed for use with polygons with potentially irregular sizes (which some of the cells have after applying the forest-only analysis mask); and 2) mgcv had extensions for non-normal response variables. The quasi-binomial family was an appropriate choice, as it allowed for overdispersion. The response variable was then framed as a number of 1-m by 1-m cells within the 20-m by 20-m cell of the DEM which were classified as 'woody cover' as binomial successes, and those classified as 'herbaceous cover' as binomial failures.

We used a variety of metrics to assess how well we accounted for spatial autocorrelation. Though Dormann et al. (2007) rejected the GAM as an adequate way to represent spatial autocorrelation, they used the default knot basis dimension (k) of 10, which was likely not to account for spatial autocorrelation in a dataset with small distances between points. Wood (2006) provided a function in mgcv called "gam.check" which gave a p-value for a test of whether k was large enough, and when tested with our dataset, gam.check indicated that a much higher k was needed. Therefore, k was set at $n/10$ (where n is the number of records), the GAM was fit with a smooth term for Northing and Easting, and the Moran test (R package "spdep," Bivand, 2013) was used to test for global autocorrelation in the model residuals. For those sites and scales which still indicated significant autocorrelation, the model was run again with $k = n/5$. We also tried a beta distribution as suggested by Schmid et al. (2013), but even at higher k values the Moran test indicated significant autocorrelation for most cell sizes. A thin plate regression spline basis, which was more typical of geographic modeling with GAMs as they are rotationally invariant, produced no appreciable changes to -parameter estimates as compared with the MRF basis (see in Appendix B).

For each site, we aggregated the data at the raster level to a range of cell sizes and fit models for each cell size. Das et al. (2011) calculated a tree's neighborhood, "an area big enough to allow at least two of the largest trees to interact," based on allometric equations for tree species in the Sierra Nevada mixed-conifer forest. They found that a 9-m radius (18-m diameter) was a reasonable area to "capture local processes affecting trees both large and small." As Douglas-fir is a major component in the densest parts of our sites, as well as a component in Sierran forests studied in Das et al. (2011), we used 18 m (rounded to 20 m for raster cell sizes) as a minimum linear distance to include neighborhood dynamics. Oak species are likely to have larger and more variable crown diameters as well as wider spacing than Douglas-fir and other conifers found in the Sierra Nevada (Burns and Honkala, 1990), so scales up to 40 or 50 m may be more appropriate as neighborhoods for the more open areas of these systems; scales larger than 50 m can be considered to reflect stand-scale dynamics. We therefore aggregated the data at the raster level to cell sizes of 20, 30, 40, 50, 60, 70, 80, 90 and 100 m, resulting in a total of 36 models. Note that we aggregated the topographic variables at each cell size from the 10-m DEM using the 'average' method (rather than median) because it has been shown to have the most predictable statistical properties (Gotway and Young, 2002); see Supplementary data for Python code to create these datasets. We hypothesized that the relationships with water retention capacity and exposure variable groups should be stronger at the neighborhood scales (20–40 m), as the topographic predictor variables lose their representation of the range and variability of moisture conditions as they are aggregated to larger cell sizes. Finally, we expected these relationships to be more apparent at the wetter sites (Iaqua Buttes and Bald Hills), as it has been shown that in drier years topography matters less for vegetation (Dorman et al., 2013); we extended this logic to drier/wetter locations.

We fit models of recent woody cover as a function of topographic variables (water retention capacity, exposure, and within-site local context), historical woody cover, and smooth functions of Northing and Easting. Note that we logit-transformed historical woody cover before standardizing it to ensure that its scale would correspond to the scale of the response variable after applying the link function. We used a quasi-binomial "distribution" for the proportion of image pixels y_i within a DEM pixel i which were classified as woody cover in the 2009 NAIP image, with a link function $logit(E[y_i]) = \eta_i$ and $Var[y_i] = \phi E[y_i]$, where ϕ was the dispersion parameter. The covariates x were linear predictors with regression coefficients β:

$$\eta_i = \beta_0 + \beta_{w.ret.cap.} x_i^{w.ret.cap.} + \beta_{exposure} x_i^{exposure} + \beta_{loc.cont.} x_i^{loc.cont.} + \beta_{histcov}\,\mathrm{logit}\left(x_i^{histcov}\right) + f(Northing_i, Easting_i) \tag{1}$$

and $f(\,)$ was a smooth function using the MRF basis. We fit models at all scales for all four sites independently, and corrected for multiple comparisons using the 'false discovery rate' method in the R function "p.adjust" (which uses the method of Benjamini and Yekutieli, 2001). See Supplementary data for R code to fit these models. To illustrate the workflow associated with the processing and classification of the imagery, gridding at the scale of the DEM, scaling up, and fitting GAMs, see Fig. 3.

3. Results

3.1. Preprocessing, classification, and model diagnostics

Root mean square error (RMSE) for orthorectification in 1-m square pixels was 8.24 for Iaqua Buttes, 4.16 for Bald Hills, 7.54 for Willow Creek, and 7.93 for Blake Mountain. We show Iaqua Buttes' imagery and classifications as an example in Fig. 4; see Appendix C for the other three sites' imagery and classifications. Accuracy for the pooled 1948 images was 95% (with a kappa statistic of 0.82), and for the 2009 images was 98% (with a kappa statistic of 0.90). See Appendix D for complete error matrices.

For all models from 20 m to 100 m, the Moran test, after increasing the number of spline knots when needed, indicated no additional spatial autocorrelation in the residuals. Dispersion as represented in the quasi-binomial's scale parameter was typically estimated to be much greater than one, indicating that the quasi-binomial was a good choice for the data's distribution and a binomial without dispersion would not have been adequate. The spatial term (the smooth function of Northing/Easting) was significant for nearly all of the site/scale combinations. See Appendix E for model diagnostics and results.

Fig. 3. Workflow. The digital elevation model (DEM) and the 2009 National Agricultural Imagery Program (NAIP) image are used to orthorectify the historical image. The DEM is also used to create topographic variables which are later grouped using principal component analysis (see text). The historical image and recent NAIP image are then each individually classified using OBIA techniques in eCognition (with the help of additional per-pixel layers, e.g., Normalized Difference Vegetation Index and texture variables; see text for details). The accuracy is assessed, and then each classified image is gridded based on the DEM's 10-m cell size; then aggregated up to 20 m through 100 m grid cells. At each scale and for each site, Generalized Additive Models are fit to explore the relationship between recent cover and previous cover, geographical coordinates, and topographic variables.

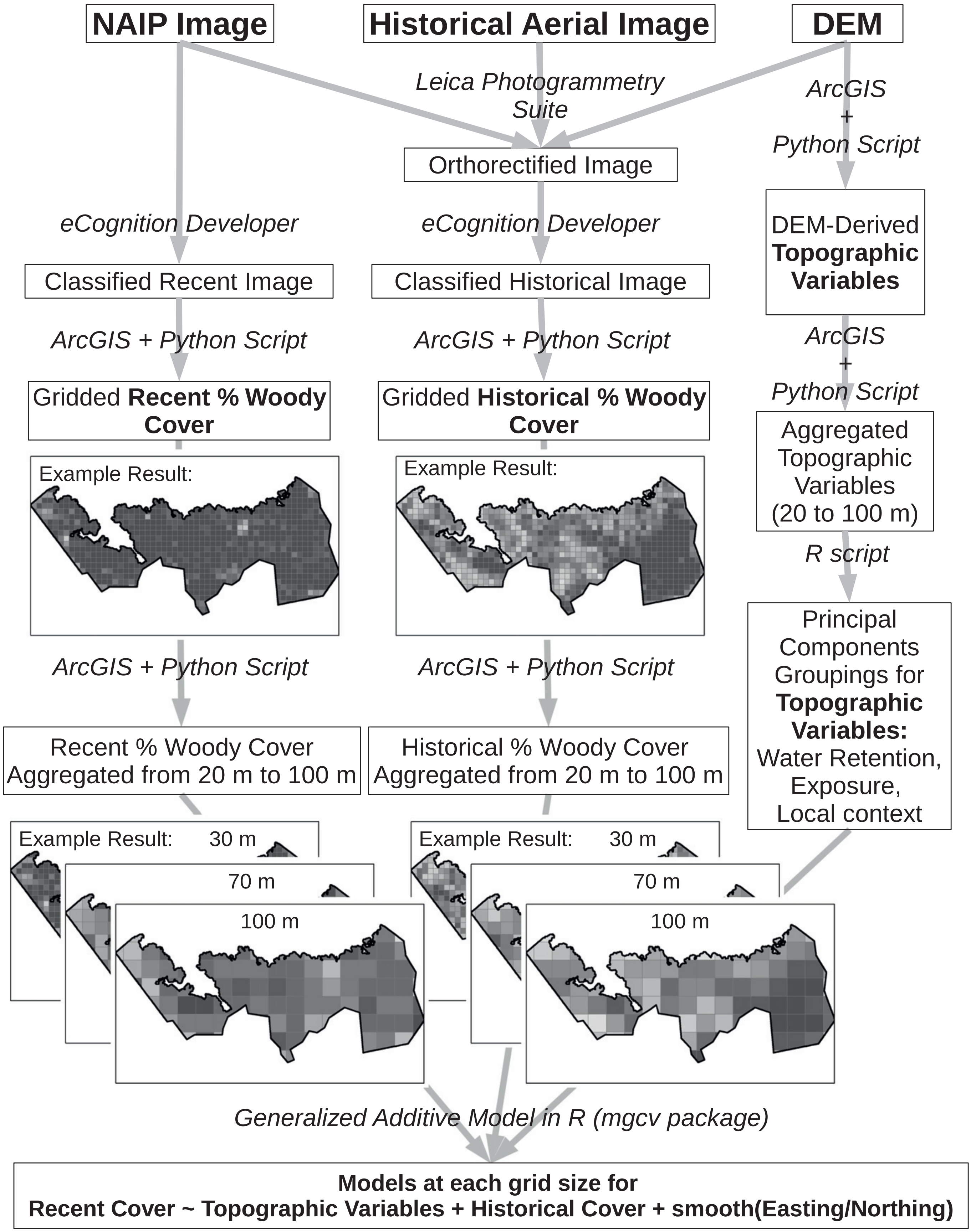
NAIP Image
Historical Aerial Image
DEM
Leica Photogrammetry Suite
ArcGIS + Python Script
Orthorectified Image
eCognition Developer
eCognition Developer
DEM-Derived Topographic Variables
Classified Recent Image
Classified Historical Image
ArcGIS + Python Script
ArcGIS + Python Script
ArcGIS + Python Script
Gridded Recent % Woody Cover
Gridded Historical % Woody Cover
Aggregated Topographic Variables (20 to 100 m)
Example Result:
Example Result:
R script
Principal Components Groupings for Topographic Variables: Water Retention, Exposure, Local context
ArcGIS + Python Script
ArcGIS + Python Script
Recent % Woody Cover Aggregated from 20 m to 100 m
Historical % Woody Cover Aggregated from 20 m to 100 m
Example Result: 30 m
70 m
100 m
Example Result: 30 m
70 m
100 m
Generalized Additive Model in R (mgcv package)
Models at each grid size for
Recent Cover ~ Topographic Variables + Historical Cover + smooth(Easting/Northing)

3.2. Sites, scales, and topographic variables

In keeping with the hypothesis of moisture limitation on forest densification, woody cover increased the most for the two wetter sites: Iaqua Buttes increased 21.3 percentage points and Bald Hills increased by 11.3 percentage points. Meanwhile, woody cover at Willow Creek increased by 1.88 percentage points, and at Blake Mountain it decreased by 1.71 percentage points.

Across sites and scales, historical woody cover was consistently significant and had a positive effect on recent woody cover. See Appendix F for means and coefficient of variation for all variables at the 10-m cell size for each site. Fig. 5 summarizes the changes in parameter estimates over different scales for each covariate. For the topographic variables, no consistent pattern between sites or scales emerged. Parameter estimates varied across cell sizes in both significance and magnitude, sometimes changing from positive to negative from one cell size to the next. See below for results of significant variables for each site. Note that the general pattern of relationships in Fig. 5 did not change when using individual variables rather than principal components, and standardizing the individual variables had little effect on the results (see Appendix G for a version of Fig. 5 with parameter estimates for a selection of the original variables, both scaled and not scaled by their standard deviations).

At Iaqua Buttes, water retention capacity had a consistently negative effect on cover, contrary to our hypothesis. However, the parameter estimate for water retention capacity variables is significant and positive at 80 m and then significant and negative at 90 m cell sizes. Though the effects of ecological variables can be expected to change over spatial scales, the reversing of the effect over a 10-m change in scale is more likely to be an artifact and indicates potential instability of the results. Local context and exposure variables are only significant for a handful of cell sizes and are unlikely to be important in reality.

Blake Mountain shows the same behavior, with the water retention capacity parameter switching from significant negative to significant positive from 90 m to 100 m. There is slightly more evidence of a negative effect (positive parameter estimate) of exposure on cover for this site (as predicted by our hypothesis), but this phenomenon is not consistent for all cell sizes within an ecological scale (neighborhood or stand level).

At Bald Hills, no topographic variables emerge as potentially significant across cell sizes, with the possible exception of exposure (though this variable also shows the negative-to-positive switch over 10 m). Of the significant parameter estimates, four of the five indicate that greater exposure results in less cover, as expected. Historical percent woody cover does appear to show a threshold, however, with previous cover having a greater impact at stand scale than neighborhood scale.

Willow Creek shows some evidence of a positive effect from water retention capacity (as expected), but only for two cell sizes. Otherwise no topographic variables are consistently important.

4. Discussion

We have tackled a number of technical problems in order to address the question of what topographic drivers influence woody cover and at what scales these influences are important. Generally, despite a dataset with many potential sources of error (including misregistration, classification error, and error associated with statistical models), as expected, the importance of controlling for historical woody cover in modeling current woody cover was clear (Fig. 5d & h). Otherwise, site- and scale-specific stories dominate the parameter estimates of the topographic variables, though there is some evidence that exposure may result in less cover for two sites (Blake Mountain and Willow Creek).

4.1. Challenges of the modeling approach

Our analysis points to several issues to consider when using historical imagery and topographic variables to predict cover change. We know that cover should not decrease at Blake Mountain (Schriver, 2015), implying that the classification uncertainty was large enough to conceal the underlying process. That site was at the eastern edge of the historical imagery so we were unable to use images to the east to constrain orthorectification. The resulting horizontal accuracy was worse at the eastern part of the site, where there was greater change but we were unable to conduct the analysis. We conclude from this that adequate imagery surrounding the image of interest is critical for reducing orthorectification error in order to conduct quantitative analyses. Though Jensen (2005) suggests that RMSE should be less than half a pixel, our overall RMSE values are within the limits of best practices according to the San Francisco Estuary Institute's historical ecology group, which frequently orthorectifies historical imagery where topography makes exact registration difficult (Micha Solomon, personal communication). Moreover, our accuracies and kappa values for the areas we did analyze were similar to other OBIA-based classifications of historical and recent imagery (Allard et al., 2012; Cserhalmi et al., 2011; Marignani et al., 2008; Martha et al., 2012; van Lier et al., 2009). Given that our accuracies and RMSEs were typical, the implication is that these methods may be better suited to situations with a robust underlying phenomenon that could be less obscured by the various sources of uncertainty, and not as useful for subtle changes in land cover.

Another limitation was the timing of the imagery: at many of our sites, tree age-structure data revealed that encroachment by Douglas-fir was already well underway by 1948 (Schriver, 2015). One possible reason that no consistent pattern in statistical models across sites emerged was that at some sites (Willow Creek, Blake Mountain) there was little total change in woody cover in our analysis areas (i.e., not enough variation in the response variable for the predictors to show a relationship). With historical remote sensing, we are restricted by the spatial and temporal availability of the imagery and this can restrict the kinds of land cover change processes we are able to study. For situations with small or subtle land cover change, this set of mapping and modeling methods may not be a good choice as the model may not detect any significant predictors when there is so little change. We also encountered difficulty in scaling this analysis up to more sites or larger areas. Like other studies (e.g., Platt and Schoennagel, 2009), we found that different strategies for classification were needed for each image and generalization was difficult: texture variables were important for the historical images and for Bald Hills in 2009, whereas NDVI was most helpful for the other recent images, and different combinations of multi-threshold segmentation and multi-resolution segmentation were most productive for different images (see Methods). In addition, pre-processing can be labor intensive and more sites or years and larger areas would require that much more analyst time.

The most important limitation highlighted by our study is the issue of the scale sensitivity of our results. Historical cover can provide a kind of ‘control’: even over 60 years, the changes in our system were slow and therefore we expected the cover from 1948 to strongly predict cover in 2009. Therefore, given that historical cover was consistently important, but not for every site and scale, we believe that our modeling strategy was appropriate for the objectives, given the above-mentioned constraints on the data and logistics. The scale sensitivity also called the use of DEM-derived variables into question. In our system, they are marginal for explaining the location of woody cover and should be used with care in similar studies. This result contrasts with Platt and Schoennagel (2009), who demonstrate some evidence for relationships between woody cover change and topographic variables across their study area; however, they do not include geographical coordinates or

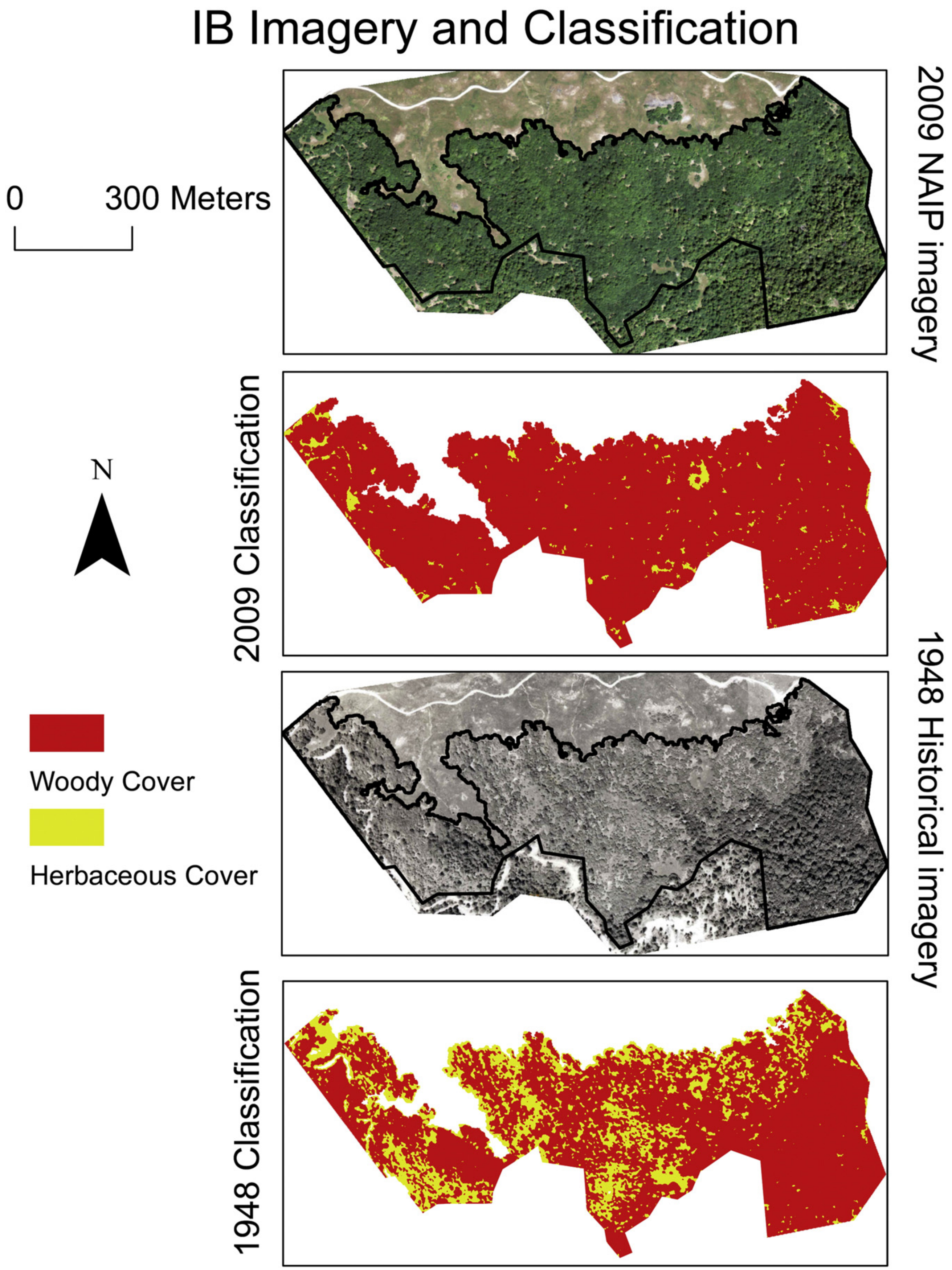

Fig. 4. Imagery and classification for the Iaqua Buttes site. Note our avoidance of the skid trails at the southern end of the image when drawing the polygon. See Appendix C for imagery and classifications for the other three sites.

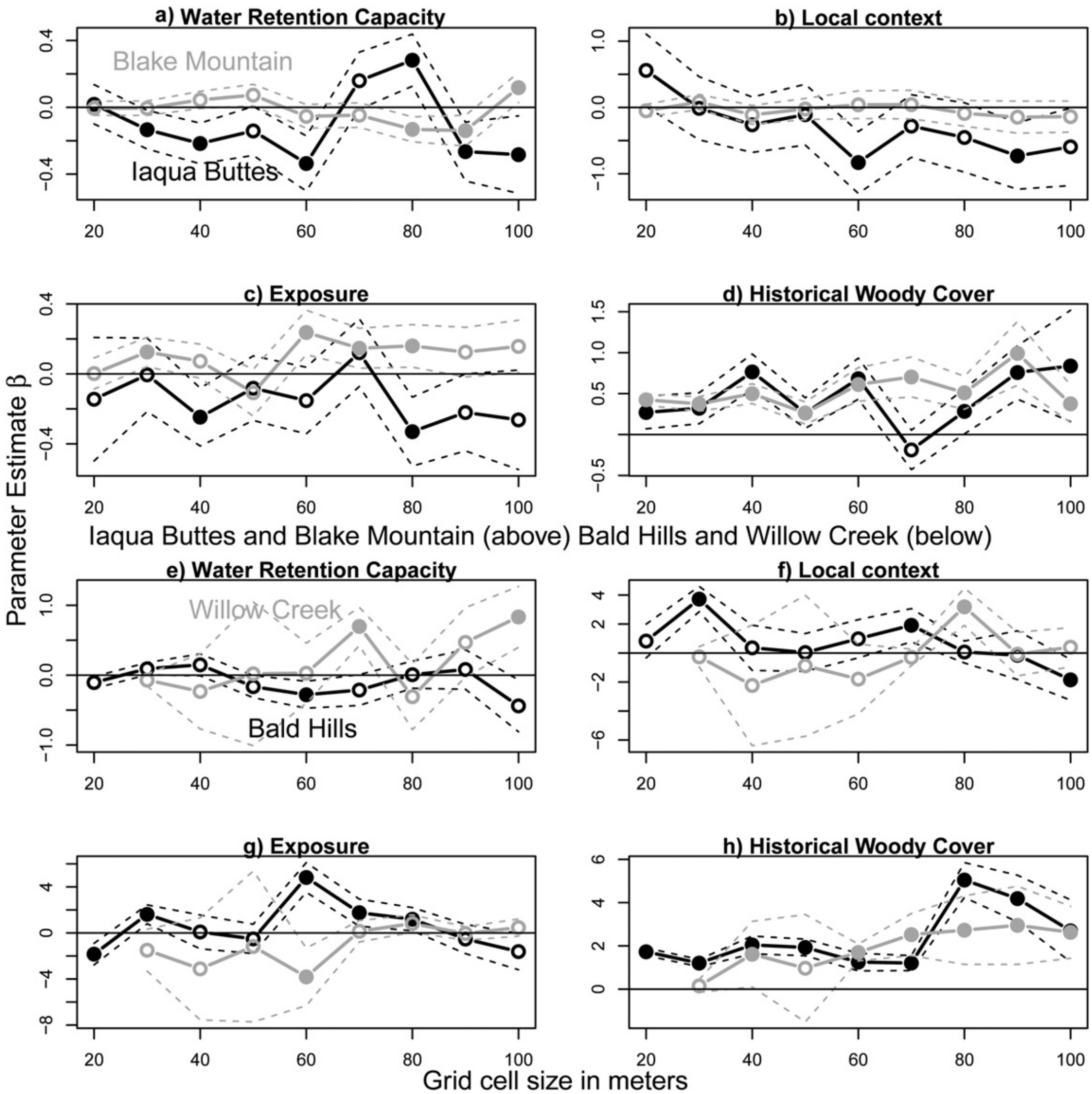

Fig. 5. Results of scaling from 20 m grid cells to 100 m grid cells for Iaqua Buttes and Blake Mountain (a through d) and Bald Hills and Willow Creek (e through h). Solid lines are associated with parameter estimates and dashed lines show 95% confidence intervals; parameter estimates which are significant at $p < 0.05$ (corrected for multiple testing) have solid circles and those that are not have open circles. Parameter estimates for a & e) water retention capacity-related variables (curvature, plan curvature, profile curvature, and slope), b & f) local (within-site) geographical context variables (elevation, distance to nearest ridge, distance to forest edge), c & g) exposure variables (insolation, eastness, northness, heat load index), and d & h) historical percent woody cover.

site factors in their model, which could shift their results. Similarly, Levick and Rogers (2011) showed some evidence that increasing topographic slope corresponds to decreased woody cover across their study area at their 10 ha and 100 ha scales, though these scales are far larger than the scales of our analysis. Newman et al. (2014b) showed some impacts of slope across their study area, but the change in woody cover in their system was due to deforestation, and slope has a strong impact on human access to forests. Our sites are also quite wet (annual rainfall between 1458 and 2782 mm) relative to sites in Israel (annual rainfall between 200 and 850 mm) where relationships between topography and vegetation growth have been shown (Dorman et al., 2013). Topography may be more important in other climatic or anthropological contexts.

Most importantly, scale sensitivity implies that if one had used only one scale (e.g., the scale of one available dataset), the conclusion would have depended strongly on which scale was used. This result argues for more frequent and rigorous investigation of scale sensitivity. We hope that the ArcGIS Python scripts developed for this research project might make this kind of scale sensitivity test more accessible for other analysts. Another solution is to compare the results with other datasets, even qualitatively, to check for spurious scale-dependent relationships. In our case, we were able to refer to dendrochronological work done on the same system (Schriver and Sherriff, 2015), but in historical ecology more generally these data sources can include historical land surveys and travel journals (Grossinger, 2012).

4.2. Opportunities of the modeling approach

Segmentation and classification strategies in eCognition are still rapidly evolving; methods and rule sets for automatically selecting segmentation parameters are under development (Dragut et al., 2010, 2014; Martha et al., 2012), but there is not yet consensus on best practices. Better classifications, which could then better capture the process of interest, may be possible as these tools develop further. Machine learning techniques are being brought together with segmentation to more automatically classify images (Nancy Thomas, personal communication). This set of approaches with historical imagery could become more powerful as new methods are developed. We do caution that even with machine learning, some supervision and validation using aerial photo interpretation techniques or other data sources are still necessary (Sexton et al., 2015).

Studies modeling historical change have used various simplifications and other strategies to account for the statistical challenges of spatial autocorrelation and the boundedness of proportions. Levick and Rogers (2011) broke up the response variable into categories of percent cover and used a Canonical Correspondence Analysis in order to model the bounded variable (percent of a certain class), but accounting for the non-normal distribution could improve the model. Platt and Schoennagel (2009) addressed nonlinear relationships by breaking the explanatory variables up into categories, but smooth functions could capture nonlinear relationships in a richer way. And whereas Cserhalmi et al. (2011) mentioned regressions without addressing autocorrelation, Newman et al. (2014a, 2014b) resampled their data to avoid it, using only a fraction of the area they classified. By using carefully parameterized generalized additive statistical models, we have addressed these statistical challenges (specifically autocorrelation and non-normality of percent cover) without simplification or data reduction. In particular, our method avoids the need to reduce data by resampling in order to avoid problems of spatial autocorrelation. Ecological data can be difficult to collect, and the image processing depicted in this study is no exception. Discarding data is particularly undesirable given the need for historical references and understanding of long term ecological processes in an era of global environmental change.

Although the GAM-based approach worked well in our study to account for spatial autocorrelation and non-normal response variables, its flexibility could be exploited even further. One reason no clear relationship between woody cover and topographic variables emerged over scales or sites could be the assumption of the linear model for those variables. A GAM could also allow smooth functions of the other variables as well as the spatial coordinates. Smooth functions could capture nonlinear relationships in a more informative way than breaking the explanatory variables up into categories as Platt and Schoennagel (2009) did. Finally, if the extent of the available imagery is large enough, analyst time is abundant, and sufficient computer power is available, the GAM can be used at larger scales (e.g., Levick and Rogers, 2011).

4.3. Underlying ecology

Conifer encroachment and consequent densification are widespread throughout the North Coast of California (Cocking et al., 2012), and have been promoted by fire exclusion and the indirect effect of economically incentivizing conifer over hardwood stewardship. Specifically, the California Forest Practice Rules for private landowners prevent profiting from removal of encroaching conifers in many cases (Valachovic et al., 2015). This densification results in less understory diversity, higher fuel loads, and loss of oaks (Hanberry et al., 2014; Knapp et al., 2013), which are ecological and cultural keystone species (Garibaldi and Turner, 2004). Unfortunately, our study of woody cover change does not reflect the underlying ecological processes in this system. We were unable to discern tree species in these images (Eitzel et al., 2015). Therefore the apparent increase in woody cover at three of the sites was only suggestive of the underlying processes dominating densification at these sites, namely encroachment of Douglas-fir into oak woodland. Possibly in future studies the use of LiDAR to distinguish taller conifers from shorter oaks may improve classification ability; similarly, multispectral imagery could help to discriminate between species. However, these solutions have no historical analog. Stereo-viewing may be possible for some historical image pairs, but quality of images varies from year to year. Finally, field samples might be combined with supervised classification techniques to assist with discerning oak from conifer. Dendrochronology through tree cores, or alternative historical imagery from a similar time period, might provide samples for the supervised classification of the historical photos.

In addition, some areas within these sites show an increase in woody cover where there are no known Douglas-fir (Schriver and Sherriff, 2015), so some of the woody cover increase was due to growth of oak trees as well as recruitment of Douglas-fir seedlings and saplings and other tree and shrub species. Without identification to species, we were unable to separate out these two mechanisms of densification, which have very different consequences for ecosystem function and species diversity. In more open sites (Bald Hills and Iaqua Buttes), the recruitment of Douglas-fir into canopy gaps could account for the greater woody cover in 2009. However, no topographic proxies for moisture accumulation or solar exposure are consistently important for those sites, so we have no intuition from these models as to what topographic factors might encourage Douglas-fir to encroach.

Generally speaking, the uniqueness of the sites' responses to these variables implies that drivers of woody cover change were very site-specific, and it is likely that additional variables would be needed to explain spatial variation at each scale. The topographic variables we explored do not consistently explain the changes in woody cover. In future work, we could explore other variables representing grazing history and soil characteristics. We could also consider a single multiscale statistical model which explicitly includes underlying processes and observation error from misclassification and misregistration (e.g., a hierarchical model incorporating observation error, Eitzel et al., 2013). We also note that we do not introduce new data at any of the scales; every cell size was aggregated up from the 10 meter scale. Future work might integrate different data sources at different scales using a hierarchical model.

5. Conclusions

Historical aerial imagery can be effectively used in quantitative statistical models, though it is a labor intensive process. Though this study, using historical and recent high spatial resolution imagery, produced inconclusive results regarding the topographic drivers of woody cover change, this simply highlights the importance of field work to document the problem and complement the historical imagery. Field validation is particularly important in an era of "Big Data" and high resolution imagery. In future remote sensing studies on this problem, higher spectral resolution may allow analysts to map species, but the process inherently involves a mixed conifer-oak class and thorough field work will still be necessary to validate models. Historical data need validation as well, whether the source of validation information comes from field work (e.g., dendrochronology), interpretation of aerial stereo photo pairs, or from historical work (e.g., travel journals and explorers' accounts). Finally, because the cell size of the analysis completely changed the conclusions from these likely marginal topographic variables, future work should perform a cell size sensitivity analysis wherever possible.

Acknowledgments

Thanks to Micha Salomon and Chuck Striplen at the San Francisco Estuary Institute for assistance with orthorectifying and georegistering historical imagery, to Madelinn Schriver and Rosemary Sherriff for field insight on the study areas, and to the Geospatial Innovation Facility at UC Berkeley (gif.berkeley.edu) for access to and support on using eCognition and Leica Photogrammetry Suite. Comments from Christopher Lee, Mary Power and John Battles improved the manuscript. University of California Agricultural and Natural Resources funded this work and the California Department of Forestry and Fire Protection scanned and provided the historical imagery.

Supplementary data

Appendices and supplementary files associated with this article can be found in the online version, at doi: http://dx.doi.org/10.1016/j.ecoinf.2015.11.011. Appendices include: the amount of principal component analysis variance explained (Appendix A), a comparison of spline smoothing choice for Iaqua Buttes (Appendix B), classifications and imagery for Bald Hills, Blake Mountain, and Willow Creek (Appendix C), error matrices for classifications (Appendix D), model diagnostics and results for all cell sizes and sites (Appendix E), summaries of response and predictor variables at the 10-m cell size for each site (Appendix F), and the results of scaling for selected individual variables (both standardized by their standard deviations and unstandardized; Appendix G). Supplementary files include: R code for calculating texture variables, for conducting accuracy assessment, and for fitting Generalized Additive Models; Python scripts to create datasets for analysis at each scale and to generate random points for accuracy assessment; eCognition rulesets for classifying two of the sites in both 1948 and 2009; a guide to orthorectification and georegistration in Leica Photogrammetry Suite; and a kmz file showing the locations of the four sites in Humboldt County.

References

Agee, J.K., 1993. Fire Ecology of Pacific Northwest Forests. Island Press, Washington, DC.
Allard, M., Fournier, R.A., Grenier, M., Lefebvre, J., Giroux, J.-F., 2012. Forty years of change in the bulrush marshes of the St. Lawrence Estuary and the impact of the greater snow goose. Wetlands 32, 1175–1188.
Beale, C.M., Lennon, J.J., Yearsley, J.M., Brewer, M.J., Elston, D.A., 2010. Regression analysis of spatial data. Ecol. Lett. 13, 246–264.
Benjamini, Y., Yekutieli, D., 2001. The control of the false discovery rate in multiple testing under dependency. Ann. Stat. 29, 1165–1188.
Betts, M.G., Ganio, L.M., Huso, M.M.P., Som, N.A., Huettmann, F., Bowman, J., Wintle, B.A., 2009. Comment on "Methods to account for spatial autocorrelation in the analysis of species distributional data: a review". Ecography 32, 374–378.
Bissonette, A., 1997. Scale-sensitive ecological properties: historical context, current meaning Chapter 1 Wildlife and Landscape Ecology: Effects of Pattern and Scale, pp. 3–31.
Bivand, R.S., 2013. Applied Spatial Data Analysis With R. Springer.
Burns, R.M., Honkala, B.H., 1990. Silvics of North America: 1. Conifers; 2. Hardwoods. U.S. Department of Agriculture, Forest Service, Washington, DC (URL http://www.na.fs.fed.us/spfo/pubs/silvics_manual/table_of_contents.htm).
Cocking, M.I., Varner, J.M., Sherriff, R.L., 2012. California black oak responses to fire severity and native conifer encroachment in the Klamath Mountains. For. Ecol. Manag. 270, 25–34.
Conchedda, G., Durieux, L., Mayaux, P., 2008. An object-based method for mapping and change analysis in mangrove ecosystems. ISPRS J. Photogramm. Remote Sens. 63, 578–589.
Cserhalmi, D., Nagy, J., Kristóf, D., Neidert, D., 2011. Changes in a wetland ecosystem: a vegetation reconstruction study based on historical panchromatic aerial photographs and succession patterns. Folia Geobotanica 46, 351–371.
Das, A., Battles, J., Stephenson, N.L., van Mantgem, P.J., 2011. The contribution of competition to tree mortality in old-growth coniferous forests. For. Ecol. Manag. 261, 1203–1213.
de Chant, T., Kelly, M., 2009. Individual object change detection for monitoring the impact of a forest pathogen on a hardwood forest. Photogramm. Eng. Remote Sens. 75, 1005–1013.
Deng, Y., Chen, X., Chuvieco, E., Warner, T., Wilson, J.P., 2007. Multi-scale linkages between topographic attributes and vegetation indices in a mountainous landscape. Remote Sens. Environ. 111, 122–134.
Deng, Y., Goodchild, M.F., Chen, X., 2009. Using NDVI to define thermal south in several mountainous landscapes of California. Comput. Geosci. 35, 327–336.
Desclée, B., Bogaert, P., Defourny, P., 2006. Forest change detection by statistical object-based method. Remote Sens. Environ. 102, 1–11.
Dorman, M., Svoray, T., Perevolotsky, A., 2013. Homogenization in forest performance across an environmental gradient — the interplay between rainfall and topographic aspect. For. Ecol. Manag. 310, 256–266.
Dormann, C.F., 2009. Response to comment on "Methods to account for spatial autocorrelation in the analysis of species distributional data: a review". Ecography 32, 379–381.
Dormann, C.F., McPherson, J.M., Araújo, M.B., Bivand, R., Bolliger, J., Carl, G., Davies, R.G., Hirzel, A., Jetz, W., Kissling, W.D., Kühn, I., Ohlemüller, R., Peres-Neto, P.R., Reineking, B., Schröder, B., Schurr, F.M., Wilson, R., 2007. Methods to account for spatial autocorrelation in the analysis of species distributional data: a review. Ecography 30, 609–628.
Dormann, C.F., Elith, J., Bacher, S., Buchmann, C., Carl, G., Carré, G., Marquéz, J.R.G., Gruber, B., Lafourcade, B., Leitão, P.J., Münkemüller, T., McClean, C., Osborne, P.E., Reineking, B., Schröder, B., Skidmore, A.K., Zurell, D., Lautenbach, S., 2013. Collinearity: a review of methods to deal with it and a simulation study evaluating their performance. Ecography 36, 27–46.
Dragut, L., Tiede, D., Levick, S.R., 2010. ESP: a tool to estimate scale parameter for multiresolution image segmentation of remotely sensed data. Int. J. Geogr. Inf. Sci. 24, 859–871.
Dragut, L., Csillik, O., Eisank, C., Tiede, D., 2014. Automated parameterisation for multi-scale image segmentation on multiple layers. ISPRS J. Photogramm. Remote Sens. 88, 119–127.
Dronova, I., Gong, P., Wang, L., 2011. Object-based analysis and change detection of major wetland cover types and their classification uncertainty during the low water period at Poyang Lake, China. Remote Sens. Environ. 115, 3220–3236.
Eitzel, M.V., Battles, J., York, R., Knape, J., de Valpine, P., 2013. Estimating tree growth from complex forest monitoring data. Ecol. Appl. 23, 1288–1296.
Eitzel, M., Kelly, M., Quinn-Davidson, L., 2015. Lessons learned in historical mapping of conifer and oak in the north coast. In: Standiford, R.B., Purcell, K.L., tech. cords (Eds.), Proceedings of the seventh California oak symposium: managing oak woodlands in a dynamic world Gen. Tech. Rep. PSW-GTR-251. U.S. Department of Agriculture, Forest Service, Pacific Southwest Research Station, Berkeley, CA, pp. 521–528 (579 p., http://www.fs.fed.us/psw/publications/documents/psw_gtr251/).
Engber, E.A., Varner III, J.M., Arguello, L.A., Sugihara, N.G., 2011. The effects of conifer encroachment and overstory structure on fuels and fire in an oak woodland landscape. Fire Ecol. 7, 32–50.
ESRI, 2013. ArcGIS URL http://www.esri.com/.
Franklin, J., 1995. Predictive vegetation mapping: geographic modelling of biospatial patterns in relation to environmental gradients. Prog. Phys. Geogr. 19, 474–499.
Garbarino, M., Lingua, E., Weisberg, P.J., Bottero, A., Meloni, F., Motta, R., 2013. Land-use history and topographic gradients as driving factors of subalpine *Larix decidua* forests. Landsc. Ecol. 28, 805–817.
Garibaldi, A., Turner, N., 2004. Cultural keystone species: implications for ecological conservation and restoration. Ecol. Soc. 9.
Gärtner, P., Förster, M., Kurban, A., Kleinschmit, B., 2014. Object based change detection of Central Asian Tugai vegetation with very high spatial resolution satellite imagery. Int. J. Appl. Earth Obs. Geoinf. 31, 110–121.
Gimmi, U., Bugmann, H., 2013. Preface: integrating historical ecology and ecological modeling. Landsc. Ecol. 28, 785–787.
Gotway, C.A., Young, L.J., 2002. Combining incompatible spatial data. J. Am. Stat. Assoc. 97, 632–648.
Grossinger, R., 2012. Napa Valley Historical Ecology Atlas: Exploring a Hidden Landscape of Transformation and Resilience. Univ of California Press.
Hanberry, B.B., Kabrick, J.M., He, H.S., 2014. Densification and state transition across the Missouri Ozarks landscape. Ecosystems 17, 66–81.
Haralick, R., Shanmugam, K., Dinstein, I., 1973. Textural features for image classification. IEEE Trans. Syst. Man Cybern. 3, 610–620.
Hawkins, B.A., 2012. Eight (and a half) deadly sins of spatial analysis. J. Biogeogr. 39, 1–9.
Herpigny, B., Gosselin, F., 2015. Analyzing plant cover class data quantitatively: customized zero-inflated cumulative beta distributions show promising results. Ecol. Inform. 26, 18–26.
Intergraph, 2012. ERDAS Imagine 2013.
Jenkins, R.B., Coops, N.C., 2011. Landscape controls on structural variation in eucalypt vegetation communities: Woronora Plateau, Australia. Aust. Geogr. 42, 1–17.
Jensen, J.R., 2005. Introductory Digital Image Processing: A Remote Sensing Perspective. 3rd edition. Pearson Prentice Hall, Upper Saddle River, NJ.
Knapp, E.E., Skinner, C.N., North, M.P., Estes, B.L., 2013. Long-term overstory and understory change following logging and fire exclusion in a Sierra Nevada mixed-conifer forest. For. Ecol. Manag. 310, 903–914.
Kuhn, I., Dormann, C.F., 2012. Less than eight (and a half) misconceptions of spatial analysis. J. Biogeogr. 39, 995–1003.
Laliberte, A.S., Rango, A., Havstad, K.M., Paris, J.F., Beck, R.F., McNeely, R., Gonzalez, A.L., 2004. Object-oriented image analysis for mapping shrub encroachment from 1937 to 2003 in southern New Mexico. Remote Sens. Environ. 93, 198–210.
Laudenslayer, W.F., Darr, H.H., 1990. Historical effects of logging on the forests of the Cascade and Sierra Nevada ranges of California. Trans. Western Sect. Wildl. Soc. 26, 12–23.
Levick, S.R., Rogers, K.H., 2011. Context-dependent vegetation dynamics in an African savanna. Landsc. Ecol. 26, 515–528.
Livingston, A.C., 2014. Plant Community Responses to Fire Exclusion, Species Invasions, and Restoration in California Woodlands and Grasslands (Master's thesis) Humboldt State University.
Marignani, M., Rocchini, D., Torri, D., Chiarucci, A., Maccherini, S., 2008. Planning restoration in a cultural landscape in Italy using an object-based approach and historical analysis. Landsc. Urban Plan. 84, 28–37.
Martha, T.R., Kerle, N., van Westen, C.J., Jetten, V., Vinod Kumar, K., 2012. Object-oriented analysis of multi-temporal panchromatic images for creation of historical landslide inventories. ISPRS J. Photogramm. Remote Sens. 67, 105–119.
Miller, J., Franklin, J., Aspinall, R., 2007. Incorporating spatial dependence in predictive vegetation models. Ecol. Model. 202, 225–242.
Morgan, J.L., Gergel, S.E., 2013. Automated analysis of aerial photographs and potential for historic forest mapping. Can. J. For. Res. 43, 699–710.
Müllerová, J., Pergl, J., Pyšek, P., 2013. Remote sensing as a tool for monitoring plant invasions: testing the effects of data resolution and image classification approach on the detection of a model plant species *Heracleum mantegazzianum* (giant hogweed). Int. J. Appl. Earth Obs. Geoinf. 25, 55–65.
Newman, M.E., McLaren, K.P., Wilson, B.S., 2014a. Assessing deforestation and fragmentation in a tropical moist forest over 68 years: the impact of roads and legal protection in the Cockpit Country, Jamaica. For. Ecol. Manag. 315, 138–152.
Newman, M.E., McLaren, K.P., Wilson, B.S., 2014b. Long-term socio-economic and spatial pattern drivers of land cover change in a Caribbean tropical moist forest, the Cockpit Country, Jamaica. Agric. Ecosyst. Environ. 186, 185–200.

Platt, R., Schoennagel, T., 2009. An object-oriented approach to assessing changes in tree cover in the Colorado Front Range 1938–1999. For. Ecol. Manag. 258, 1342–1349.
Pringle, R.M., Syfert, M., Webb, J.K., Shine, R., 2009. Quantifying historical changes in habitat availability for endangered species: use of pixel- and object-based remote sensing. J. Appl. Ecol. 46, 544–553.
R Development Core Team, 2009. R: A Language and Environment for Statistical Computing.
Sanderson, E., 2009. Mannahatta: A Natural History of New York City. Abrams, New York, NY.
Schmid, M., Wickler, F., Maloney, K.O., Mitchell, R., Fenske, N., Mayr, A., 2013. Boosted beta regression. PLoS One 8, e61623.
Schriver, M.R., 2015. Stand and Tree Growth Characteristics of *Quercus garryana* and *Quercus kelloggi* Woodlands in Northwestern California (Master's thesis) Humboldt State University.
Schriver, M., Sherriff, R., 2015. Tree establishment in Oregon white oak and California black oak woodlands in northwestern California. In: Standiford, R.B., Purcell, K.L., cords, tech. (Eds.), Proceedings of the seventh California oak symposium: managing oak woodlands in a dynamic world. Gen. Tech. Rep. PSW-GTR-251. U.S. Department of Agriculture, Forest Service. Pacific Southwest Research Station, Berkeley, CA, pp. 529–540 (579 p., http://www.fs.fed.us/psw/publications/documents/psw_gtr251/).
Seidl, R., Eastaugh, C.S., Kramer, K., Maroschek, M., Reyer, C., Socha, J., Vacchiano, G., Zlatanov, T., Hasenauer, H., 2013. Scaling issues in forest ecosystem management and how to address them with models. Eur. J. For. Res. 132, 653–666.
Sexton, J.O., Noojipady, P., Anand, A., Song, X.-P., McMahon, S., Huang, C., Feng, M., Channan, S., Townshend, J.R., 2015. A model for the propagation of uncertainty from continuous estimates of tree cover to categorical forest cover and change. Remote Sens. Environ. 156, 418–425.
Stoddard, M.A., Hayes, J.P., 2005. The influence of forest management on headwater stream amphibians at multiple spatial scales. Ecol. Appl. 15, 811–823.
Stow, D., Hamada, Y., Coulter, L., Anguelova, Z., 2008. Monitoring shrubland habitat changes through object-based change identification with airborne multispectral imagery. Remote Sens. Environ. 112, 1051–1061.
Swetnam, T.W., Allen, C.D., Betancourt, J.L., 1999. Applied historical ecology: using the past to manage for the future. Ecol. Appl. 9, 1189–1206.
Thysell, D.R., Carey, A.B., 2001. Manipulation of density of *Pseudotsuga menziesii* canopies: preliminary effects on understory vegetation. Can. J. For. Res. 31, 1513–1525.
Trimble, 2013. eCognition Developer.
Valachovic, Y., Quinn-Davidson, L., Standiford, R.B., 2015. Can the California Forest Practice Rules adapt to address conifer encroachment? In: Standiford, R.B., Purcell, K.L, cords, tech. (Eds.), Proceedings of the seventh California oak symposium: managing oak woodlands in a dynamic world. Gen. Tech. Rep. PSW-GTR-251. U.S. Department of Agriculture, Forest Service. Pacific Southwest Research Station, Berkeley, CA, pp. 515–520 (579 p., http://www.fs.fed.us/psw/publications/documents/psw_gtr251/)
van Lier, O.R., Fournier, R.A., Bradley, R.L., Thiffault, N., 2009. A multi-resolution satellite imagery approach for large area mapping of ericaceous shrubs in Northern Quebec, Canada. Int. J. Appl. Earth Obs. Geoinf. 11, 334–343.
Wang, Y., Hou, X., Wang, M., Wu, L., Ying, L., Feng, Y., 2013. Topographic controls on vegetation index in a hilly landscape: a case study in the Jiaodong Peninsula, eastern China. Environ. Earth Sci. 70, 625–634.
Warton, D.I., Hui, F.K.C., 2011. The arcsine is asinine: the analysis of proportions in ecology. Ecology 92, 3–10.
Whipple, A.A., Grossinger, R.M., Davis, F.W., 2011. Shifting baselines in a California oak savanna: nineteenth century data to inform restoration scenarios. Restor. Ecol. 19, 88–101.
Wood, S.N., 2006. Generalized Additive Models: An Introduction With R. Chapman & Hall/CRC, Boca Raton, FL.
Zvoleff, A., 2014. glcm: Calculate Textures from Grey-level Co-occurrence Matrices (GLCMs) in R URL http://cran.r-project.org/package=glcm.